PROCEEDINGS OF SPIE

SPIEDigitalLibrary.org/conference-proceedings-of-spie

Imaging performance of the Hobby-Eberly Telescope

Palunas, Povilas, MacQueen, Phillip, Booth, John, Calder, Robert, Fowler, James, et al.

Povilas Palunas, Phillip J. MacQueen, John A. Booth, Robert Calder, James R. Fowler, Matthew D. Shetrone, Stephen C. Odewahn, Pedro Segura, Gordon L. Wesley, George Damm, Jerry Martin, P. Samuel Odoms, "Imaging performance of the Hobby-Eberly Telescope," Proc. SPIE 6267, Ground-based and Airborne Telescopes, 62673V (23 June 2006); doi: 10.1117/12.672700

Event: SPIE Astronomical Telescopes + Instrumentation, 2006, Orlando, Florida , United States

Imaging Performance of the Hobby-Eberly Telescope*

Povilas Palunas†, Phillip J. MacQueen, John A. Booth, Robert Calder, James R. Fowler, Matthew D. Shetrone, Stephen C. Odewahn, Pedro Segura, Gordon L. Wesley, George Damm, Jerry Martin, P. Samuel Odoms
McDonald Observatory, University of Texas at Austin, 1 University Station C1402, Austin, TX 78712, USA

ABSTRACT

The HET is a modified Arecibo-style telescope with a segmented spherical primary and a four-mirror spherical aberration corrector (SAC). Objects are tracked by driving the SAC along the focal sphere of the primary. In the original design of the telescope the alignment of the SAC was to be maintained passively. In practice, this could not be done to specifications, leading to degraded imaging quality. We have developed a metrology system to actively control the alignment of the SAC. An autocollimator maintains the optical axis of the SAC normal to the primary mirror beneath it. An absolute distance measuring interferometer (DMI) monitors the SAC/primary mirror distance, maintaining focus. Both systems work at a wavelength of 1.5 microns, well above the operating wavelength of current or planned science instruments and therefore do not interfere with observations. The performance of the system is measured via Hartmann testing.

Several upgrades are implemented in the primary mirror control system, including calibration of individual edge sensors, new control system software, and a new method of setting and controlling the overall radius of curvature of the primary array. New techniques were developed to efficiently piston the segments onto the proper sphere radius.

Keywords: Telescopes: Hobby-Eberly

1. INTRODUCTION

The Hobby-Eberly Telescope (HET)[1,2] is a fixed elevation telescope with an 11 m segmented spherical primary mirror array. The HET design employs an Arecibo-style spherical primary and focal surface robot which tracks objects in the sky. The final image is formed by a 4-mirror double-Gregorian spherical aberration corrector (SAC) which rides in the tracker prime focus instrument package (PFIP). The telescope, which is tilted 35° from zenith, can be rotated in azimuth to access different regions of the sky between observations, but remains stationary during observations.

The HET is the prototype for extremely cost-effective large telescopes. The telescope was built for only $13.9 M, about 15% of the cost of a fully-steerable telescope of comparable size. Cost-savings measures were pushed to the extreme and the telescope fell short of specifications. In early operations the typical delivered image quality was 2.5-3.0 arcsec FWHM and observing efficiency was poor[3]. A concentrated effort was launched to understand and address these problems with additional funding. Two of the most significant contributors to the poor performance were the primary mirror[3,4] and the tracker robot[3,5]. Both of these critical and highly complex opto-mechanical systems were being run open loop and could not maintain specified alignment tolerances.

To maintain good image quality the tracker must maintain the optical alignment of the SAC at the proper distance from and normal to the primary mirror as it tracks objects across the focal sphere. SAC tip and tilt errors with respect to the primary lead to coma and distance errors lead to defocus. Ideally these errors would be measured directly via a wavefront sensor. The relatively small (4′) field of the current HET SAC precludes this. We have developed a tracker

---

* The Hobby – Eberly Telescope is operated by McDonald Observatory on behalf of the University of Texas at Austin, The Pennsylvania State University, Stanford University, Ludwig-Maximillians-Universität München, and Georg-August-Universität, Göttingen.

† P.P: E-mail: palunas@astro.as.utexas.edu

Ground-based and Airborne Telescopes, edited by Larry M. Stepp, Proc. of SPIE
Vol. 6267, 62673V, (2006) · 0277-786X/06/$15 · doi: 10.1117/12.672700

metrology system to allow precision alignment of the SAC frame during observations. The system consists of an auto-collimator called the tip-tilt camera (TTCAM) and a distance measuring interferometer (DMI) both working in the near-infrared. The tracker metrology system is currently undergoing on telescope commissioning.

The primary mirror is aligned with a Shack-Hartmann sensor located in the center of curvature tower. The mirror alignment recovery system[6] (MARS) measures the relative tip tilt errors of the images of a projected spot for the individual primary mirror segments. MARS has been operational since October 2001 and regularly achieves the 0.065" rms segment tip tilt error specification. Remaining issues with the primary mirror alignment have been setting the global radius of curvature (GRoC) and the relative piston of individual segments. A DMI has recently been installed on MARS to efficiently set the GRoC to within 20 μm. New procedures have been developed to set the piston with errors of less than 5μm and maintain it to errors to less than 20 μm rms. Operational efficiency has also been improved with the MARS system, with typical restacks taking about 30 minutes under normal conditions.

The alignment of the 91 segments in the primary mirror array degraded significantly on timescales of under an hour due to thermally driven deformations in the underlying bolted steel support truss. To correct this shortfall an edge sensor system, the Segment Alignment Maintenance System[78] (SAMS) was procured to close the loop on the primary mirror control system. SAMS was contracted to NASA Marshall Space Flight Center and Blue Line Engineering in November 1999 and the system went into initial operation starting in January 2002. The system provided an immediate improvement to HET operations by reducing the number of required array realignments, or stacks, of the primary to just 2 or 3 per night.
Control of the primary mirror has steadily improved through better calibration of the SAMS sensors. Currently the stacking rate is 1.4 stacks per night requiring a total of about 4% of night time operations.

Over the past 2 years all of the primary mirror segments have been recoated with aluminum coatings. During this time the segments were set-up optimally on their mounts using new fixturing. Evaluation of the segment figure at the center of curvature with the Hartmann Extra-Focal Imager[9] (HEFI) shows that the more carefully set up mounts have eliminated instances of very poor figure. The aluminum coatings have also substantially improved the telescope throughput[10].

2. TRACKER METROLOGY SYSTEM

In conventional telescopes the optics are mounted in a rigid structure and require relatively small corrections to maintain alignment against gravitational and thermo-elastic loading. On the HET, however, the optical alignment must be held dynamically while the image moves as much as 3.8 m with respect to the main telescope structure along the focal sphere. Furthermore the mechanisms controlling the tracker do not act along natural axes. Motions along the focal sphere are synthesized from x, y, focus (z), tip (θ), tilt (ϕ), rotation (ρ) axes controlled from stacked x and y stages, a hexapod system and a rotation stage.

To track an object and maintain good image quality the motion of the SAC must be controlled in all six degrees of freedom to strict tolerances using 10 encoded actuators. The range of motion for each axis is: 3800 mm in x and y, 130 mm in z, 18° in θ and ϕ, and 200° deg in ρ. During a track, the PFIP rotates in ρ (up to +/-19.4° in the north) to maintain a fixed position angle on the sky. In the original design of the telescope the only feedback to control the motion with respect to the primary mirror was provided by a guider which constrained only the two pointing degrees of freedom. The remaining degrees of freedom were to be modeled.

To overcome the deficiencies of the mount-models we have developed a metrology system to enable closed-loop feedback on focus, tip and tilt of the PFIP with respect to the primary mirror. Focus is measured with an absolute distance measuring interferometer (DMI) while tip and tilt are measured with an auto-collimator system called the tip-tilt camera (TTCAM). A similar system was adopted by SALT[11]. Both the DMI and TTCAM operate at a wavelength of 1.5 μm which is outside the range of any current or planned instrument used on the HET.

2.1 DMI

The DMI is a low-coherence distance measuring interferometer developed by Fogale-Nanotech[12,13]. The operation of the system is based on a pair of Michelson interferometers in which all of the optical paths, excepting the measurement arm, are along optical fibers (Figure 1). The first interferometer encodes the phase difference to the primary mirror with respect to a reference at the collimator measurement head, a distance equal to 2LM. The two arms of the second interferometer induce phase delays of 2(LR1+LS) and LR2 respectively, where LS is adjustable via an optically encoded scanning mirror. The second interferometer reads the phase difference from the coding interferometer by scanning through the exact phase matching condition where LR1+LS-LR2 = LM.

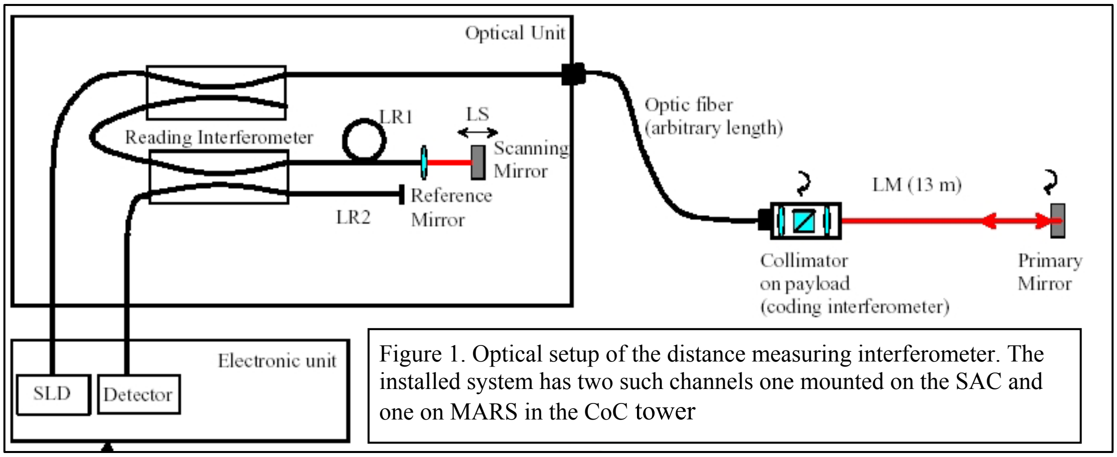

Figure 1. Optical setup of the distance measuring interferometer. The installed system has two such channels one mounted on the SAC and one on MARS in the CoC tower

This configuration allows the compact measurement head of the instrument to be mounted remotely. The optical fiber feeding the measurement head can be of arbitrary length. The distance measurement is unaffected by thermally induced changes to the length of feed fiber. The reading interferometer is housed in a thermally controlled chamber to maintain stability.

The system light source is a poly-chromatic super-luminescent diode (SLED). An interference signal is detected only when the phase difference is less than the coherence length of the source and is modulated by a peaked function called the visibility curve. Figure 2 shows an example of an interference curve. The peak of the visibility curve occurs at the exact phase matching condition of LR1+LS-LR2 = LM. The absolute distance is obtained by finding the peak. Even if the beam is temporarily interrupted the measurement is not affected as for laser based distance measuring interferometers. The range of the scanning mirror is 40 mm which allows a comfortable range for locating and setup of the measurement head.

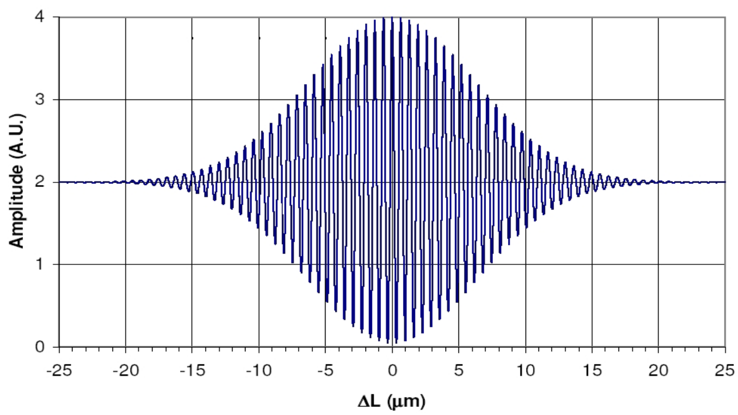

Figure 2 Example interference curve for polychromatic source

The scanning mirror covers the 40 mm scanning distance in 5 sec. In practice the upper range of the motion has been limited to reduce the measurement time. The visibility curve is sampled in 10 ms and therefore normal movement of the measurement head does not affect the measurement signal. The RMS repeatability of measurements is 1 µm over time scales several minutes. The long term accuracy is specified at 1 ppm.

The system installed at the HET has two channels one set to measure a nominal distance of approximately 12.6 m, located at the SAC, and used for tracker metrology. The other channel is set to measure a nominal distances of approximately 26.2 m to measure distances at the center of curvature.

The user interface is written in Labview.

2.2 Tip/Tilt Camera

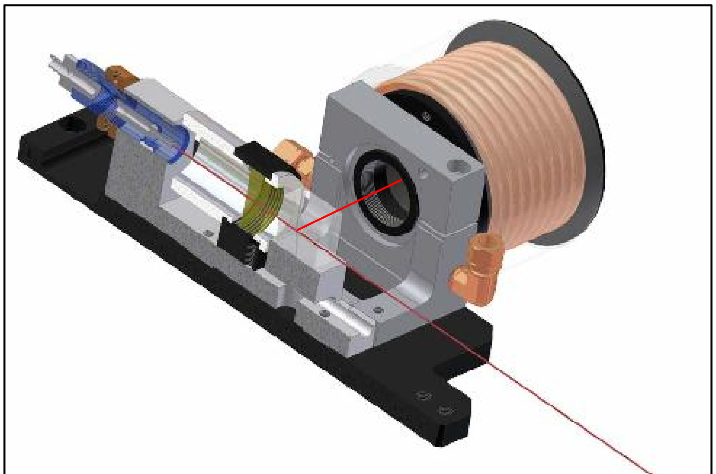

Figure 3 Cutaway diagram of the tip tilt camera. The beam path is shown in red.

The TTCAM (Figure 3) was developed in house as we could not locate a commercial product operating in the near infra-red which met our specifications for accuracy, stability and capture range. The system projects a beam at a normal to the primary mirror and the return beam is routed through a beam-splitter to a camera with a phosphor coated CCD yielding a diffraction limited spot size of 2 mm. The only optics in the system are: a collimator lens for the source, the beam-splitter, and a long pass filter in front of the camera. The system provides a capture range of ±75" and an rms centroiding repeatability of 0.2". Optical modeling shows that HET images degrade by 0.5" FWHM due to coma for 25" tip tilt errors of the SAC.

The 1.5 µm source is fiber fed though a SMF-28 single mode fiber which emits a beam with a smooth Gaussian beam profile with no additional spatial filtering. The beam is collimated by a one inch diameter, 50 mm focal length, achromatic doublet lens optimized for the near infrared from Thor labs. The primary mirror focuses the beam back onto the CCD camera.

The camera utilized is a Pulnix 1020 with a 1k x 1k CCD with 9 µm pixels, 8-bit digital conversion and a 15 Hz readout rate. The CCD was coated with an anti-Stokes up-conversion phosphor by Spiricon Inc. The phosphor produces visible photons at a rate of roughly the square of the input signal and has a threshold power of 3 mW (Figure 4). The camera has a total dynamic range of only a factor of two, which is sufficient for our purposes. The long pass filter in front of the camera prevents both visible light from outside the camera from contributing to the background signal on the CCD and also prevents the glow of the phosphor from escaping the camera during observations.

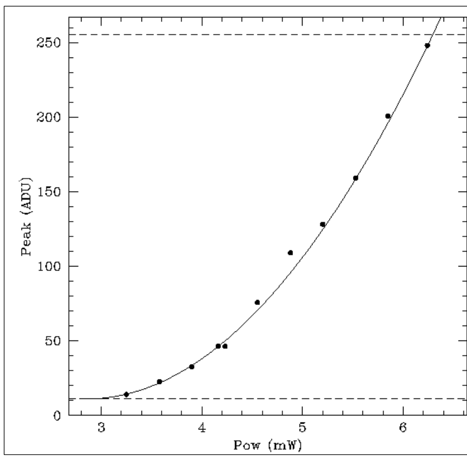

Figure 4. Peak camera response as a function of source input power. A 3m W threshold combined with the quadratic response function leads to a total dynamic range of only 2x.

The camera is controlled by a PCI DV FOX digital camera interface from Engineering Design Team, Inc. This interface provides a fiber link that allows remote placement of the control computer.

The light source is a fiber-coupled amplified spontaneous emission (ASE) source from Lightwaves2020. The source has a spectral width of 50 nm, which eliminates problems with fringing due to a laser source (Figure 5).

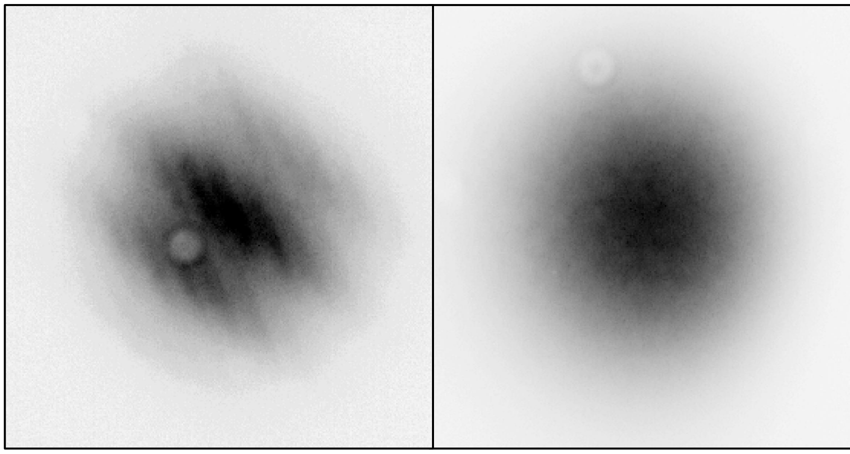

Figure 5 Left: spot from a laser source. Right: spot from a the non-coherent ASE source. The laser source has multiple interference patterns due to wedged surfaces in the long-pass filter. Occasionally, a little incoherence can be a good thing.

The mounts for the TTCAM must maintain a high degree of stability: a 250 nm lateral displacement of the end of the source fiber yields a 1" tip/tilt error. The TTCAM optical bench and mounting brackets are machined from Invar 36 to provide a stable platform for the instrument. It is mounted rigidly to the SAC structure which is fabricated from 5/8" diameter Invar 36 rod. The TTCAM is mounted as close to the SAC gimbal and centerline axis as possible, while still allowing access for adjustment and maintenance. The fiber end is mounted in an Invar 36 cylinder with a focusing mechanism. Only the ceramic ferrule and strain relief boot of a standard FC connector are used. The ferrule is axially spring loaded and epoxied into body of this assembly for maximum stability. The assembly provides adjustments to do the initial pointing of the instrument. The camera is mounted to a clamp is made from stainless steel which is ported for glycol circulation. This was required because the CCD, one of the primary heat sources, is rigidly attached to the aluminum front end of the camera. A copper tubing coil assembly, through which glycol is also circulated, surrounds the remainder of the camera

2.3 Hartmann testing

The tracker metrology system provides measurements of the distance, tip and tilt of the SAC optics mounting structure with respect to primary mirror. This provides a much more direct measurement than the strain path through all the tracker mechanisms and the telescope structure. However, it still does not provide the direct measurement of what we care about: the wavefront arriving at the telescope focal plane. In order to set the TTCAM zero-point and test for flexure between the TTCAM and the SAC optical axis we performed Hartmann testing. A Hartmann mask was placed at the exit pupil of the telescope near the last mirror in the SAC optical train. The Hartmann mask was configured with 4 mm diameter holes on 12.75 mm centers in a 15x15 grid. This puts several spots on an illuminated primary mirror segment at any given time. The diffraction limited spot size for each aperture is 1.4" at the focal plane. A spare guiding and acquisition camera was mounted to a special fixture, the Hartmann test fixture (HTF), which allowed sufficient focal depth, 60 mm, to resolve the individual Hartmann spots. Guiding during the tests was done with standard HET acquisition camera fed from a pellicle below prime focus.

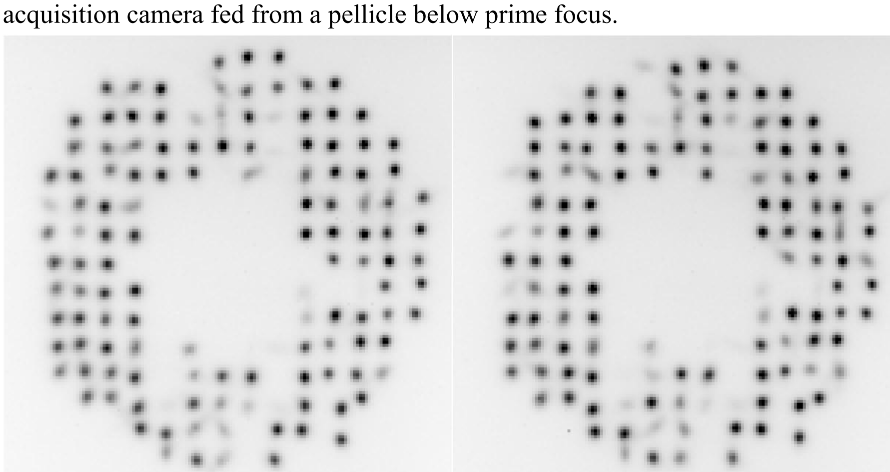

Figure 6 Left Hartmann image with SAC tip tilt errors of 40". Right: Hartmann image for a flat wavefront with minimal coma.

Figure 6 shows examples of the Hartmann data with a tilted (comatic) wavefront and with a corrected wavefront. Software was developed to reduce the data in real time and yield tip, tilt, and focus corrections for the SAC. The main results of the Hartmann tests were that initial tip tilt errors of the SAC using the mount model were variable and as large as 90". The Hartmann data allowed corrections to within 3" rms in tip and tilt. Once the wavefront was corrected the guide camera yielded images of 1.5" FWHM, consistent with the diffraction limit of the individual Hartmann spots, stack size and DIMM seeing.

To test for flexure, rho offsets were put in. This causes a substantial redistribution of the weight on the PFIP. At each offset the guider was recentered the wavefront was flattened and then TTCAM tip tilt position measured. This measurement was done on multiple tracks over two nights with rho offsets made in random order during the track. It was found that the SAC had substantial internal flexure (Figure 7) of up to 60" at rho offset of -50°. The flexure was found to be very repeatable. A subsequent investigation of the SAC found broken flex pivots for the counterweight system supporting the M3 mirror at the lower end of the SAC.

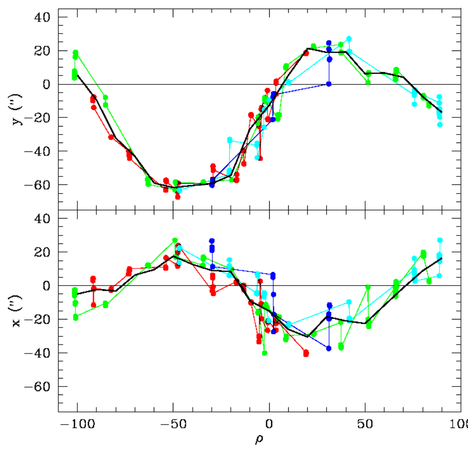

Figure 7 Position of spot on TTCAM as a function of tracker ρ after the SAC was aligned to yield images with negligible coma. The colors indicate data taken during different tracks. The black line is the smoothed position for all of the data.

Further Hartmann testing will be done once these flexures are replaced

3. PRIMARY MIRROR IMAGE QUALITY

3.1 Stacking

The global radius of curvature (GRoC) of the primary mirror must match the average segment radius of curvature to optimize the imaging of the telescope. A 1 mm error in the GRoC leads to 0.41" blur in an image. During stacking the GRoC is determined by the distance of the MARS instrument from the primary mirror. Previously this distance was set by knife edge focusing on a single segment representative of the average radius of curvature. This method proved to have poor accuracy, was time consuming, and required the subjective intervention of the telescope operator. Because of the difficulties in performing the knife edge it was generally done only at the beginning of the stack and the subsequent thermal contraction of the tower during the stack was not tracked. Errors in the GRoC of the stack amounted to 500 µm rms and occasionally were found to be well in excess of 1mm.

To improve the accuracy of the system and aid in automation of stacking a DMI was installed on the MARS system in the CoC tower. The MARS DMI is an additional channel in the same system that houses the SAC DMI described above. The only difference is that the lengths of the legs in the reading interferometer are set to read distances close to 26.2 m near the average radius of the primary mirror segments.

The MARS DMI which gives 20 µm absolute accuracy eliminates the GRoC problem. The system is integrated into the stacking software and automatically sets the position of MARS with respect to the at every stack iteration.

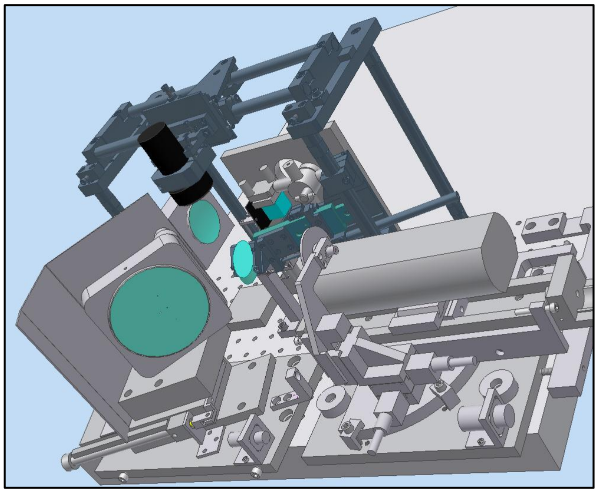

Figure 8. MARS DMI. The DMI measurement head (black) is held rigidly on a support structure above the main MARS instrument. A pickoff mirror on a pneumatic slide is placed on the optical axis of the primary mirror to measure the distance from MARS to the primary.

3.2 Primary Mirror Segment Piston

The relative radial error of the individual segment from the fiducial primary mirror sphere is called the segment piston. The HET imaging error budget allows 25 μm rms piston error. Segment piston in the array was set manually with a hand-held spherometer every several months. The procedure was labor intensive and subject to error as the spherometer physically contacted the segments.

We have developed a technique to measure the relative piston of the segments using the SAC DMI. The tracker is set up to make short trajectories along the focal sphere such that the DMI beam crosses the gap between segments. DMI measurements are made throughout each trajectory so that multiple distance measurements are made on either side of the gap. The timing between measurements is set up so that at least one measurement falls in the gap to give an unambiguous indication that the segments have been straddled. The difference between the measurements on one segment versus those on the adjacent segment gives the relative piston error. Because the measurements are differential the tracker errors are minimized. Measurements are made between every pair of adjacent segments and the relative piston is solved through a set of simultaneous equations connecting all of the measurements. The measurements overconstrain the problem (240 measurement and 90 degrees of freedom) which allows a consistency check against bad measurements. Using this method the relative piston can be set to 3 μm rms error.

To maintain the piston we have begun using the SAMS edge sensor system measurements. The long term stability of the sensors is not sufficiently good to maintain the overall figure of the primary mirror. Furthermore, sensor errors tend to induce low order modes in the primary starting with astigmatism. These lowest order modes tend to allow the largest piston errors. This problem can be eliminated, however, because we are able to constrain the segment tip/tilt degrees of freedom after we perform a stack. By comparing two SAMS references taken after stacking and solving for only the relative piston degrees of freedom we are able to mitigate piston errors over a much longer time scale.

3.3 SAMS

The SAMS edge sensor system has been very robust. We have been able to iterate on the calibration of the sensors and achieve steadily improving performance. To evaluate the performance of SAMS the stack is measured using HEFI subsequent to every stack. The stack is remeasured prior to restacking or at the end of the night. The degradation in the stack is measured by subtracting the initial stack measurement in quadrature from the final stack measurement. In Figure 9 we plot this metric for operations over the past 9 months. In October 2005 and April 2006 new SAMS sensor

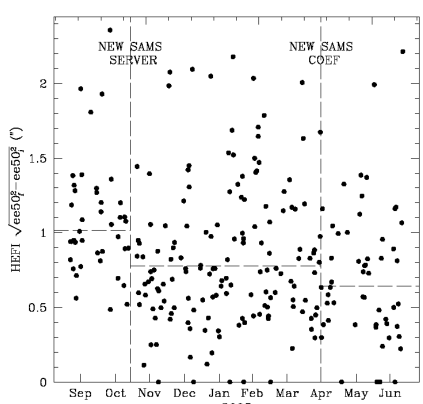

Figure 9. SAMS performace over the past 9 months. The performance metric is explained in the text. The annotated activities each show an improvement in SAMS performance.

calibration coefficients were installed.

A new software server controlling the SAMS system was released in October 2005. The new server has graphical interface which provides substantially more feedback for the telescope operators to evaluate the state of the system and allow efficient reconfiguration to remove bad sensors. In addition the algorithm controlling the primary GRoC was changed. The prior algorithm used 4 segments fixed in piston to define the GRoC. Errors in controlling these segments introduced global errors in tip, tilt and radius of curvature of the primary. In the new server the control equations are solved by singular value decomposition and these global modes are removed from the control equations. GRoC corrections needed due to thermal expansion of the truss are estimated based on gap measurements at the SAMS sensors and the corrections are added open loop after the control equations.

In April 2005 a new primary mirror control server, the segment control system (SCS) was released. This system controls the actuators that maintain the segment tip tilt and piston. SCS has put control of the primary mirror on a more reliable modern linux computing platform. Communication with the actuator controllers was substantially parallelized leading to substantially improved segment control performance. Updating the state of the mirror now takes 20 seconds compared to 60 seconds for the old control system. This has lead to faster stacks and better closed loop control of the primary mirror.

Overall the degradation of the stack has gone from approximately 1″ EE50 between stacks to approximately 0.6″ EE50 between stacks; which is an improvement of 80% when we consider the quadrature difference.

3.4 Segment Figure

Imaging of the primary mirror at center of curvature with the segments "burst" into a hexagonal pattern highlights figure problems with some of the mirror segments (Figure 10 left). These imaging problems are associated with specific segment support problems. Each primary mirror segment is mounted on a steel frame designed to support a segment radially through its center of mass by a flexure-mounted hub and axially on three whiffletrees (Figure 11). The flexure permits the hub to move with the mirror as it is positioned in tip, tilt, and piston while maintaining radial support at the mirror's center of mass. Tip, tilt and piston of a segment are controlled by a stepper-motor driven actuator through a compound lever system that provides 19 nm resolution in the axial travel of the whiffletrees.

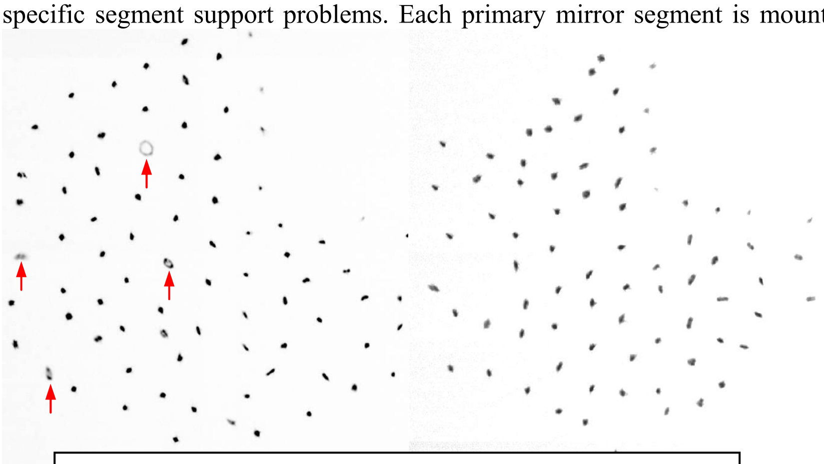

Figure 10. Best focus hexburst of primary mirror array for analysis of individual segments Left 2004, Right May 2006

The worst case figures were invariably caused by failure of the hub flexure. This was caused by embrittlement of the flexure material. Another leading cause of flexure failure was the shearing of the flexure when the mirror was moved axially beyond the travel limits of the flexure. This occurred routinely when an actuator was retracted during the homing process.

Stops were designed and have been installed to limit the travel of the mirror when the actuators were homed. New tooling and gauging hardware has been designed, built and used to properly setup each support frame to receive a mirror. The worst case segment figures have all been repaired. The new mount setups have increased the average segment radius of curvature by about 0.5 mm. Many segments still show astigmatic figure errors which are below the HET error specs. The average segment EE50 is currently 0.4" at the optimal focus for the primary mirror.

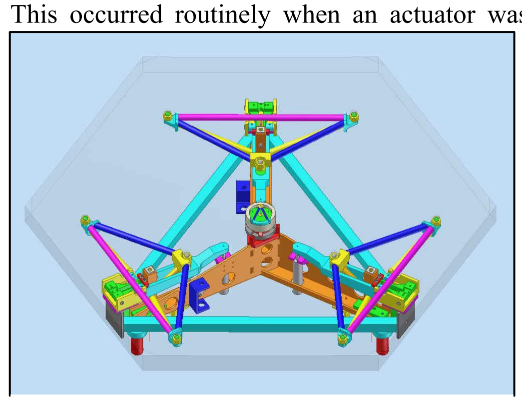

Figure 11. HET segment support

4. SUMMARY

We are completing a series of upgrades that we expect will bring the HET to its original image quality specifications. The most recent and currently most significant of these is the Tracker Metrology System (TMS) which consists of a absolute distance measuring interferometer (DMI) and an autocollimator called the tip tilt camera (TTCAM). Errors in the positioning of the SAC have been found to be a major contributor to degraded image quality. The TMS provides direct metrology for the positioning of the SAC with respect to the primary mirror array.

Additional improvements have been made in the control of the primary mirror array. Improvements in the SAMS edge sensor calibration and feedback loop have lead to an improvement of 80% in performance in the past 9 months. The SCS system has provided higher bandwidth and reliability in control of the primary mirror.

A DMI was also incorporated in the MARS system used for stacking the primary mirror and has lead to substantially better control of the primary mirror GRoC, as well as more efficient operation.

Improvements in the setup of segment mounts have yielded more consistent segment figure. Hexburst analysis shows that the current figure of the individual segments is within specs, yielding images sizes of 0.4" EE50, but that low order figure errors remain.

Over the past year the HET has delivered a median image quality of 1.6" FWHM in 1.1" FWHM site seeing measured by a DIMM.

REFERENCES

1. L.W. Ramsey, M.T. Adams, T.G. Barnes, J.A. Booth, M.E. Cornell, J.R. Fowler, N.I. Gaffney, J.W. Glaspey, J. Good, P.W. Kelton, V.L. Krabbendam, L. Long, F.B. Ray, R.L. Ricklefs, J. Sage, T.A. Sebring, W.J. Spiesman, and M. Steiner, 1998, “The early performance and present status of the Hobby-Eberly Telescope,” S.P.I.E. Vol. 3352, Advanced Technology Optical/IR Telescope VI, p.34
2. J.A. Booth, M.J. Wolf, J.R. Fowler, M.T. Adams, J.M. Good, P.W. Kelton, E.S. Barker, P. Palunas, F.N. Bash, L.W. Ramsey, G.J. Hill, P.J. MacQueen, M.E. Cornell, & E.L. Robinson, “The Hobby-Eberly Telescope Completion Project”, in Large Ground-Based Telescopes, Proc SPIE 4837, paper 109, 2002
3. G. J. Hill, “The Hobby Eberly Telescope : Instrumentation and Current Performance,” in Optical and IR Telescope Instrumentation and Detectors, Proc. SPIE 4008, 50, 2000
4. V.L. Krabbendam, T.A. Sebring, F.B. Ray & J.R. Fowler, “Development and performance of Hobby-Eberly Telescope 11-m segmented mirror,” in Advanced Technology Optical/IR Telescopes VI, Proc. SPIE 3352, 436, 1998
5. J. A. Booth, F. B. Ray, and D. S. Porter, “Development of a star tracker for the Hobby Eberly Telescope”, in Telescope Control Systems III, Proc. SPIE, 3351, 298, 1998
6. M.J. Wolf, M. Ward, J.A. Booth, A. Wirth, G.L. Wesley, D. O’Donoghue, & L. Ramsey, “Mirror Alignment Recovery System on the Hobby-Eberly Telescope”, in Large Ground-Based Telescopes, Proc SPIE 4837, 714, 2003
7. J.A. Booth, M.T. Adams, G.H. Ames, J.R. Fowler, E.E. Montgomery, J.M. Rakoczy, “Development of the segment alignment maintenance system (SAMS) for the Hobby-Eberly Telescope”, Proc. of SPIE, 4003, 176, 2000
8. J.M. Rakoczy, D Hall, W. Ly, R.T. Howard, E.E. Montgomery, M.T. Adams, J.A.Booth, J.R. Fowler, G.H. Ames, “Primary mirror figure maintenance of the Hobby-Eberly Telescope using the Segment Alignment Maintenance System”, Proc. of SPIE, 4837, 702, 2003
9. P. Palunas, J.R. Fowler, J.A. Booth, G. Ames, G. Damm, “Control of the Hobby-Eberly Telescope primary mirror array with the segment alignment maintenance system,” *Proc. SPIE*, **5496**, 659, 2004.
10. J.A. Booth, et al. “The Hobby-Eberly Telescope: performance upgrades, status and plans,” Proc. SPIE, 5489, 288, 2004
11. G. J. Hill, P.J. MacQueen, P. Palunas[a], M. D. Shetrone, & J. A. Booth, “Present and Future Instrumentation for the Hobby-Eberly Telescope”, Proc. SPIE, 6269, paper 6269-05, 2006
12. D.A.H. Buckley, G.P. Swart, J.G. Meiring, “Completion of the Southern African Large Telescope”, Proc. SPIE, 6267, paper 6267-19, 2006
13. A. Koch, R. Ulrich, "Fiber-optic displacement sensor with 0.02 m resolution by white-light interferometry", Sensors and actuators. A, Physical, vol. 25 no.1-3, pp. 201-207, 1991
14. A. Courteville, F. Garcia & L. Nel, “Positioning of Optical Payload – SALT Telescope” , Proc. SPIE, 5495, 463